# Mimicking salmochelin S1 and the interactions of its Fe(III) complex with periplasmic iron siderophore binding proteins CeuE and VctP

Ellis J. Wilde,[a, b] Elena V. Blagova,[a] Thomas J. Sanderson,[b] Daniel J. Raines,[b] Ross P. Thomas,[b] Anne Routledge,[b] Anne-Kathrin Duhme-Klair[b]* and Keith S. Wilson[a]*

[a] Structural Biology Laboratory, Department of Chemistry, University of York, Heslington, York YO10 5DD, UK

[b] Department of Chemistry, University of York, Heslington, York YO10 5DD, UK

* Correspondence to: Anne-Kathrin Duhme-Klair, Department of Chemistry, University of York, York YO10 5DD, UK. Tel: 01904 322587, email: anne.duhme-klair@york.ac.uk; Keith S. Wilson, Structural Biology Laboratory, Department of Chemistry, University of York, York YO10 5DD, UK. Tel: 01904 328262, Fax: 01904 328266, e-mail: keith.wilson@york.ac.uk, https://www.york.ac.uk/chemistry/

Dedicated to Prof. Bernt Krebs on the occasion of his 80th birthday

## Graphical Abstract

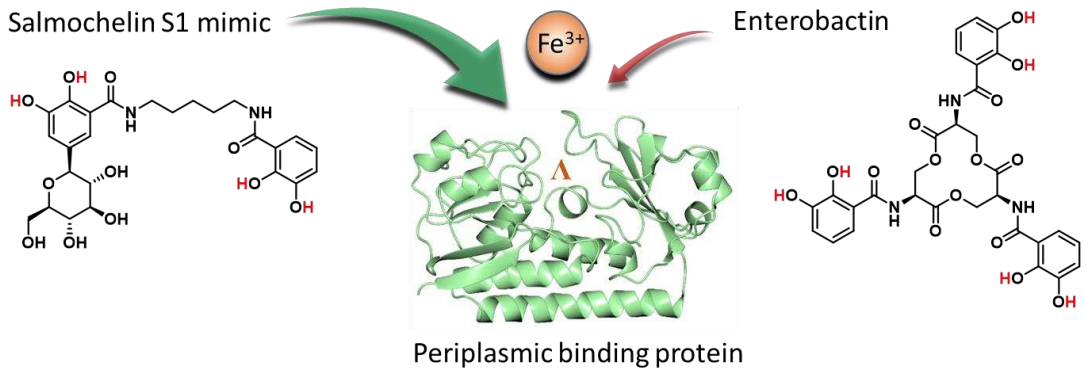


The periplasmic binding protein VctP of *Vibrio cholerae*, binds the Fe(III) complexes of a tetradentate salmochelin S1 mimic with higher affinity than does the periplasmic binding protein CeuE of *Campylobacter jejuni*. Both proteins select for Λ-configured Fe(III) complexes and display a preference for bis(catecholates) over the tris(catecholate) siderophore enterobactin.

## Highlights

- Synthesis of a mimic of the tetradentate stealth siderophore salmochelin S1
- The periplasmic binding protein of *Vibrio cholerae* (VctP) binds the mimic strongly
- VctP selects for Λ-configured Fe(III) complexes of the mimic
- VctP displays a preference for bis(catecholate) over tris(catecholate) siderophores
- The role of salmochelin in iron uptake by pathogens merits further investigation

## Abstract

A mimic of the tetradentate stealth siderophore salmochelin S1, was synthesised, characterised and shown to form Fe(III) complexes with ligand-to-metal ratios of 1:1 and 3:2. Circular dichroism spectroscopy confirmed that the periplasmic binding proteins CeuE and VctP of *Campylobacter jejuni* and *Vibrio cholerae*, respectively, bind the Fe(III) complex of the salmochelin mimic by preferentially selecting Λ-configured Fe(III) complexes. Intrinsic fluorescence quenching studies revealed that

VctP binds Fe(III) complexes of the mimic and structurally-related catecholate ligands, such as enterobactin, bis(2, 3-dihydroxybenzoyl-L-serine) and bis(2, 3-dihydroxybenzoyl)-1, 5-pentanediamine with higher affinity than does CeuE. Both CeuE and VctP display a clear preference for the tetradentate bis(catecholates) over the tris(catecholate) siderophore enterobactin. These findings are consistent with reports that *V. cholerae* and *C. jejuni* utilise the enterobactin hydrolysis product bis(2, 3-dihydroxybenzoyl)-*O*-seryl serine for the acquisition of Fe(III) and suggest that the role of salmochelin S1 in the iron uptake of enteric pathogens merits further investigation.

**Key words:** Salmochelin, Stealth Siderophore Mimic, Iron Uptake, *Vibrio cholerae,* Periplasmic Binding Protein

# Introduction

Iron is an essential element required for the survival and growth of bacteria within a host organism. Iron(II) is in scarce supply in aerobic environments, so iron(III) must be taken up, despite its poor aqueous solubility of $10^{-18}$-$10^{-17}$ mol dm$^{-3}$ at pH 7.[1] Requiring concentrations between $10^{-8}$ and $10^{-6}$ mol dm$^{-3}$ for growth,[2] complex strategies must be employed by bacteria for acquisition of sufficient iron for survival.[1, 3] Siderophores are low molecular weight (<1500 Da) compounds with high affinity for iron(III) that are produced, secreted and employed by bacteria for iron(III) uptake.[2, 4] *Vibrio cholerae* acquires essential iron by producing the catecholate siderophore vibriobactin, and by poaching enterobactin and its linear hydrolysis products from competing bacteria in the surrounding environment (

Figure and scheme captions:

Figure 1).[5-8]

In response, some host organisms produce siderocalins which can bind a number of iron(III)-bound siderophores, including enterobactin and vibriobactin, with subnanomolar dissociation constants, and hinder bacterial iron(III)-siderophore uptake.[9-15] However, due to the specificity of the siderocalin binding pocket, some functionalised enterobactin derivatives, and siderophores with structural differences

cannot be bound.[9, 16, 17] Such stealth siderophores are therefore able to evade the host immunoprotein siderocalin, allowing for more effective iron acquisition.[16-19] Examples include the salmochelin siderophores, which are *C*5-glucosylated analogues of enterobactin, and its hydrolysis products, produced by pathogenic strains of *Escherichia coli* (Figure 2).[20-23] They have high iron(III) affinity, but are more hydrophilic than enterobactin, with the glucose units providing steric bulk.[24, 25] These two properties allow the siderophores to avoid sequestration by siderocalin.[26, 27]

*V. cholerae* can colonise the mammalian gut, where enterobactin and vibriobactin are sequestered by siderocalins.[15-18, 28] Due to the high pathogenicity of *Vibrio cholerae*, estimated to cause at least 120,000 global deaths per year,[29, 30] we were particularly interested to investigate whether this species is capable of employing salmochelin-type stealth siderophores.

While a number of previous studies on the use of iron(III)-enterobactin in *V. cholerae* did not consider the potential presence of enterobactin hydrolysis products, such as tris(2, 3-dihydroxybenzoyl-L-serine) (trisDHBS), bis(2, 3-dihydroxybenzoyl-L-serine) (bisDHBS) and 2, 3-dihydroxybenzoyl-L-serine (DHBS), recent studies give a more complete picture of enterobactin-derived iron(III) acquisition.[7, 31-34] Whilst it remains unclear whether or not intact cyclic enterobactin can support growth of *V. cholerae*, it is now accepted that iron(III)-trisDHBS and iron(III)-bisDHBS provide efficient iron(III) delivery pathways.[34, 35] TonB, a protein that enables the active transport of essential nutrients, is required for the transport of iron(III)-siderophore complexes across the outer membrane *via* the two outer membrane receptor proteins VctA and IrgA for linear enterobactin derivatives,[36] and the receptor for vibriobactin ViuA (Figure 3).[31, 37, 38] Both periplasmic-binding protein dependent ABC transporters VctPDGC and ViuPDGC have been shown to transport iron(III)-vibriobactin and iron(III)-enterobactin derivatives into the cytoplasm. Crystal structures have been reported for periplasmic binding proteins VctP and ViuP: VctP in the apo form (PDB ID: 3TEF), and ViuP with vibriobactin bound (PDB ID:3R5T).[39,4]

Our previous studies on the periplasmic binding protein CeuE from *Campylobacter jejuni*, which binds the tetradentate siderophore iron(III)-bisDHBS, revealed a strong similarity between CeuE and VctP.[41, 42] VctP shares sequence similarities (25.3%

identical, 47.6% similar residues) and high structural similarities (r.m.s.d of 1.78 Å over 263 Cα positions, 100% match for secondary structure elements PDB ID: 3ZKW, 3TEF) with CeuE. Both proteins contain conserved histidine and tyrosine residues that complete coordination of the iron(III) centre of tetradentate siderophore complexes in CeuE.[41-43] It is proposed that VctP has an analogous function to CeuE, and is optimised for binding tetradentate iron(III)-siderophore complexes. We here proceed to establish the siderophore-binding properties of VctP, to further understand its exact role in iron-uptake in *V. cholerae*. A number of catecholate siderophores and siderophore mimic compounds were screened for their binding affinity with VctP. A tetradentate salmochelin mimic was synthesised, its iron-binding properties characterised, and its interaction with CeuE and VctP evaluated. This study aimed to reveal whether these periplasmic binding proteins could be involved in uptake of Fe(III)-salmochelin S1 (Figure 2). This is the first indication that *V. cholerae* may employ salmochelin-type siderophores as an iron-uptake strategy that evades host siderocalin.

# 1 Materials and Methods

## 1.1 Siderophores and siderophore mimics

Enterobactin was obtained from EMC microcollections (Tübingen) and used as supplied after compound purity was confirmed by HPLC and extinction coefficient determination. Bis(2, 3-dihydroxybenzoyl-L-serine) (bisDHBS) and bis(2, 3-dihydroxybenzoyl)-1, 5-pentanediamine (5-LICAM) were synthesised as previously reported.[42, 43]

## 1.2 Instrumentation

NMR spectra were recorded on Jeol EX and ES 400 MHz instruments. $^{1}H$ experiments were run at 399.78 MHz. $^{13}C$ experiments were run at 100.53 MHz and were proton decoupled. Positive and negative ion electrospray ionisation mass spectrometry (ESI-MS) was performed on a Bruker microTOF electrospray mass spectrometer. Elemental analysis was performed on an Exeter CE-440 elemental analyser. Infrared (ATIR) spectra were recorded on a Perkin Elmer FT-IR spectrum two spectrophotometer at ambient temperature. Melting points were determined using a Stuart Scientific SMP3 melting point apparatus. Specific rotation was

recorded on a Jasco DIP-370 digital polarimeter. Fluorescence spectra were recorded on a Hitachi F-4500 fluorescence spectrophotometer at ambient temperature. Electronic absorption spectra were recorded on a Shimadzu UV-1800 spectrophotometer at ambient temperature. Circular dichroism was performed on a Jasco J810 CD spectropolarimeter at 20 °C under a constant flow of nitrogen.

## 1.3 Synthesis of salmochelin mimics

Methoxy-5-aceto-β-D-glucosyl-3, 4-benzyloxysalicylate (**5**),[44, 45] 2, 3-bis(benzyloxy)benzoic acid (**9**)[46] and 2, 3-bis(benzyloxy)benzoic acid N-hydroxysuccinimide ester (**10**)[47] were prepared as documented in the literature. Compound structures with the atom numbering scheme used for the NMR assignments are available in the Supporting Information.

### 1.3.1 Methyl-5-iodo-3-methoxysalicylate (2)

Methyl-5-iodo-3-methoxysalicylate was prepared as in the literature, replacing the o-vanillin substrate for **5**.[48] The crude product was recrystallised from a minimum amount of hot ethanol. (2.379 g, 7.72 mmol, 73%) $R_f$ = 0.50 (1:4 ethyl acetate : petroleum ether 40-60°C) M.P = 109-111 °C. **$^1$H NMR:** (400 MHz, $CDCl_3$) δ: 10.99 (s, *H*9, 1H); 7.76 (d, *J*= 2.0 Hz, *H*4/6, 1H); 7.25 (d, *J*= 2.0 Hz, *H*4/6, 1H); 3.96 (s, *H*10, 3H); 3.89 (s, *H*8, 3H). **$^{13}$C NMR:** (100 MHz, $CDCl_3$) δ: 169.6 (*C*7); 152.0, 149.3, 114.2 (*C*1, 2, 3); 129.5, 124.9 (*C*4,6); 56.4 (*C*8); 52.7 (*C*10). **HRMS (ESI):** Calcd. $[M+H]^+$ ($C_9H_9IO_4$) m/z = 308.9618; Obs. $[M+H]^+$ m/z = 308.9629, Mean err 3.7 ppm. Calcd. $[M+Na]^+$ ($C_9H_9INaO_4$) m/z = 330.9438; Obs. $[M+Na]^+$ m/z = 330.9446, Mean err 2.9 ppm. **IR ATIR (cm$^{-1}$):** 3090 br w (C-H), 2943 w (C-H), 1674 m (C=O), 1607 m (C=C ar), 1471 s (C-H), 1343 m (O-H).

### 1.3.2 Methyl-5-iodo-3-hydroxysalicylate (3)

Methyl-5-iodo-3-hydroxysalicylate was prepared by adaptation of a literature protocol.[49] Methyl-5-iodo-3-methoxysalicylate (2.000 g, 6.49 mmol) was dissolved in anhydrous dichloromethane (10 mL) and the mixture was stirred whilst the reaction flask was purged with $N_2$. $BBr_3$ (1 M in dichloromethane, 12 mL, 12.00 mmol) was added dropwise with vigorous stirring. The reaction flask was then purged again with $N_2$ and the mixture stirred overnight at room temperature. The reaction mixture was opened to air, cold $H_2O$ (20 mL) was carefully added and the reaction mixture stirred for 1 hour. The resulting pale pink turbid mixture was dissolved in methanol (20 mL)

and the solvent removed *in vacuo* yielding a red residue. Methanol (10 mL × 3) was added to the residue, the residue dissolved, and the solvent removed *in vacuo*. The resulting peach coloured solid was redissolved in methanol (50 mL) and concentrated $H_2SO_4$ (2 mL) and heated under reflux overnight. The reaction mixture was cooled to room temperature and the solvent removed *in vacuo*, yielding a colourless oil and a white solid. The residue was dissolved in ethyl acetate (150 mL) and was washed with saturated $NaHCO_3$ (3 x 90 mL) and brine (2 x 90 mL). The organic portion was dried over $MgSO_4$, filtered and the solvent removed *in vacuo* yielding a white solid (1.710 g, 5.82 mmol, 89%) $R_f$ = 0.47 (1:4 ethyl acetate : petroleum ether 40-60 °C) M.P = 136-138 °C (Lit. 133-134 °C). **HRMS (ESI):** Calcd. $[M+Na]^+$ ($C_9H_9INaO_4$) m/z = 316.9281; Obs. $[M+Na]^+$ m/z = 316.9282, Mean err 0.5 ppm. Calcd. $[M+2Na]^+$ ($C_9H_9INa_2O_4$) m/z = 338.9101; Obs. $[M+2Na]^+$ m/z = 338.9099, Mean err 0.2 ppm. **$^1$H NMR, $^{13}$C NMR, HRMS (ESI): consistent with literature data.**[44]

### 1.3.3 Methyl-5-iodo-3, 4-benzyloxysalicylate (4)

Methoxy-5-benzyloxy-5-iodo-3, 4-benzyloxysalicylate was prepared based on a literature protocol.[44,45] The residue was dissolved in 1:1 chloroform : ethyl acetate (10 mL) and purified by flash column chromatography (1:9 ethyl acetate : petroleum ether 40-60°C) followed by recrystallisation in a minimum amount of chloroform and an excess of petroleum ether 40-60°C. The white needle crystals were collected and dried *in vacuo* (1.613 g, 3.40 mmol, 78%) $R_f$ = 0.37 (1:9 ethyl acetate : petroleum ether 40-60 °C) M.P = 103-105 °C (Lit. 105-106 °C). **HRMS (ESI):** $[M+K]^+$ ($C_9H_9INKO_4$) m/z = 512.9960; Obs. $[M+K]^+$ m/z = 512.9957, Mean err 0.1 ppm. **$^1$H NMR, $^{13}$C NMR, HRMS (ESI): consistent with literature data.**[44]

### 1.3.4 Methoxy-5-benzyloxy-β-D-glucosyl-3, 4-benzyloxysalicylate (6)

Methoxy-5-benzyloxy-β-D-glucosyl-3, 4-benzyloxysalicylate was prepared based on a literature protocol.[44, 45] Methoxy-5-aceto-β-D-glucosyl-3, 4-benzyloxysalicylate (1.314 g, 1.94 mmol) was dissolved in dry methanol (100 mL) and $Na_2CO_3$ (1.026 g, 9.68 mmol) was added. The resulting suspension was stirred under reflux at 65°C overnight, then reduced *in vacuo* to a pale brown solid. The solid was transferred to a Schlenk tube, and NaH (533 mg, 60% in mineral oil, 13.3 mmol) was added. The solids were dried *in vacuo* for two hours, before the addition of DMF (25 mL) and cooling of the solution to 0 °C. $Bu_4NI$ was dried *in vacuo* for 15 minutes, to which,

benzyl bromide (3.00 mL, 4.320 g, 25.26 mmol) and DMF (5 mL) were added. The solution was cooled to 0 °C for 5 minutes, and was then added dropwise to the methyl-5-aceto-β-D-glucosyl-3,4-benzyloxysalicylate solution over 5 minutes at 0 °C. After 5 minutes of stirring at 0 °C, the pale brown reaction mixture was stirred at RT under $N_2$ overnight. The reaction mixture was opened to air, and deionised water (40 mL) carefully added. The resulting solution was extracted with ethyl acetate (3 × 50 mL). The organic portions were combined and dried over $MgSO_4$, filtered and solvent removed *in vacuo* to yield a white solid. The solid was purified by column chromatography 20% ethyl acetate in petroleum ether 40-60°C yielding the product as a white solid (0.719 g, 0.82 mmol, 42%) $R_f$ = 0.20 (20% ethyl acetate in petroleum ether 40-60°C) M.P = 84-86 °C. **HRMS (ESI):** Calcd. $[M+Na]^+$ ($C_{56}H_{54}NaO_9$) m/z = 893.3660; Obs. $[M+Na]^+$ m/z = 893.3655, Mean err 0.6 ppm. **$^1$H NMR, $^{13}$C NMR, HRMS (ESI): consistent with literature data.**[44]

### 1.3.5 Benzyloxy-5-benzyloxy-β-D-glucosyl-3, 4-benzyloxysalicylate (7)

Benzyloxy-5-benzyloxy-β-D-glucosyl-3, 4-benzyloxysalicylate was prepared by the same method as methyl-5-benzyloxy-β-D-glucosyl-3,4-benzyloxysalicylate. The compounds were then separated by column chromatography yielding the product as a white solid. (0.381 g, 0.40 mmol, 21%) $R_f$ = 0.26 (1:4 ethyl acetate : petroleum ether 40-60°C) M.P = 104-106 °C. **$^1$H NMR:** (400 MHz, $CDCl_3$) δ: 7.52 (d, *H*6, J = 1.7 Hz, 1H) 7.40-7.28 (m, *H*10, *H*15, *H*26-28, *H*31-33, *H*36-38, *H*41-43, *H*46-48, 29H); 7.26-7.21 (m, *H*4, *H*11, *H*16, 5H) 6.94-6.92 (m, *H*12, *H*17, 2H) 5.34 (d, *H*44, J = 12.4 Hz, 2H); 5.07 (d, *H*8, J = 10.1 Hz, 2H); 4.98 (d, *H*13, J = 2.2 Hz, 2H); 4.97-4.87 (m, *H*24/29, *H*39, 3H) 4.66-4.57 (m, *H*24/29/*H*23, 3H); 4.43 (d, *H*23, J = 10.1 Hz 1H); 4.21 (d, *H*18, J = 9.5 Hz, 1H); 3.82-3.76 (m, *H*20/21/24/29, *H*34, 5H); 3.61-3.59 (m, *H*22, 1H); 3.44 (t, *H*19, J = 9.0 Hz, 1H). **$^{13}$C NMR:** (100 MHz, $CDCl_3$) δ: 165.9 (*C*7); 152.5 (*C*3); 148.0 (*C*2); 138.6 (*C*25); 138.2, 138.1, 137.4, 137.2, 136.3, 135.9, (*C*1/10/15/30/35/41/45); 128.6, 128.5, 128.4, 128.4, 128.4, 128.3, 128.2, 128.2, 128.1, 128.1, 128.0, 127.9, 127.9, 127.9, 127.8, 127.8, 127.7, 127.7, 127.6, 127.6, 127.6, 126.4 (*C*5/10-12/15-17/26-28/31-33/36-38/42-44/46-48); 122.0 (*C*6); 116.5 (*C*4); 86.6 (*C*20/21); 83.9 (*C*19); 80.9 (*C*18); 79.3 (*C*22); 78.2 (*C*20/21); 75.6 (*C*8); 75.1 (*C*24/29/34); 73.2 (*C*23); 70.9 (*C*39); 68.9 (*C*24/29/34); 68.1 (*C*13); 66.9 (*C*44). **HRMS (ESI):** Calcd. $[M+Na]^+$ ($C_{62}H_{58}NaO_9$) m/z = 969.3973; Obs. $[M+Na]^+$ m/z = 969.3982, Mean err 1.3 ppm.

### 1.3.6 1-Amino-5-(2,3-dibenzyloxybenzamide) pentane (11)

1, 5-Diaminopentane (1.427 g, 14.00 mmol) and triethylamine (1.396 g, 13.80 mmol) were dissolved in THF (120 mL). A solution of 2, 3-bis(benzyloxy)benzoic acid N-hydroxysuccinimide ester (3.008 g, 6.97 mmol) in THF (60 mL) was added dropwise over 2 hours and the mixture was left to stir overnight. The solvent was removed *in vacuo* yielding an off-white solid which was taken up in chloroform (120 mL) and washed with $NaHCO_3$ (100 mL), brine (100 mL) and 2.25:1 1M HCl: brine (130 mL). The organic layer was dried over $MgSO_4$, filtered and the solvent removed *in vacuo*. The residue was purified *via* silica column chromatography (90:10:1 $CHCl_3$: MeOH: $NH_3$(aq)). (1.859 g, 59 %) $R_f$ = 0.18 (90:10:1 $CHCl_3$: MeOH: $NH_3$(aq)) M.P = 133-134 °C. **$^1$H NMR:** (400 MHz, $CDCl_3$) δ: 7.99 (t, J = 5.5 Hz, *H*8, 1H); 7.73-7.71 (m, H6/4, 1H); 7.49-7.35 (m, *H*11-13, *H*16-18, 10H); 7.16 (d, J= 2.3 Hz, *H*6/4, 2H); 7.14 (t, J= 4.6 Hz, *H*5, 1H); 5.16 (s, *H*9/14, 2H); 5.08 (s, *H*9/14, 2H); 3.27 (dd/q, J= 6.0 Hz J = 13.3 Hz, *H19*, 2H); 2.77 (t, J= 6.6 Hz, *H*23, 2H); 1.48 (dt , J= 7.3 Hz, *H*20, 2H); 1.37-1.20 (m, *H*21, *H*22, 4H). **$^{13}$C NMR:** (100 MHz, $CDCl_3$) δ: 165.0 (*C*7); 151.7, 146.7, 136.4, 128.7, 128.6, 128.6, 127.7 (*C*1-3/10-13/15-18); 124.4 (*C*4/6); 123.3 (*C*4/6); 116.7 (*C*5);76.3, 71.2 (*C*9,14); 42.0 (*C*23); 39.6 (*C*19); 33.3, 29.1, (*C*20/22); 24.2 (*C*21). **HRMS (ESI):** Calcd. $[M+H]^+$ ($C_{25}H_{29}N_2O_3$) m/z = 405.2173; Obs. $[M+H]^+$ m/z = 405.2168, Mean err 3.5 ppm. **IR ATIR (cm$^{-1}$):** 3365 m (N-H), 307b m br (N-H), 2803 m br (C-H), 1641 m (C=O), 1571 m (C=C ar).

### 1.3.7 Benzyloxy-β-D-glucosyl-3, 4-benzyloxysalicylate (12)

5-Benzyloxy-β-D-glucosyl-3,4-benzyloxysalicylate was prepared as in the literature.[44, 45] Purification involved the addition of petroleum ether 40-60 °C (3 × 10 mL) and removal *in vacuo* to yield an off white solid residue. The residue was purified by column chromatography (1:4 methanol : chloroform) yielding a white solid product (0.359 g, 0.42 mmol, 87%) $R_f$ = 0.56 (1:9 methanol : chloroform) M.P = 97-99 °C. **HRMS (ESI):** Calcd. $[M+Na]^+$ ($C_{55}H_{52}NaO_9$) m/z = 879.3504; Obs. $[M+Na]^+$ m/z = 879.3522, Mean err 2.4 ppm. **$^1$H NMR**, **$^{13}$C NMR**, **HRMS (ESI): consistent with literature data.**[44]

### 1.3.8 5-Benzyloxy-β-D-glucosyl-bis(3, 4-benzyloxy)-5-LICAM (13)

5-Benzyloxy-β-D-glucosyl-3, 4-benzyloxysalicylate (0.252 g, 0.29 mmol) was dissolved in DMF (10 mL) to which 1-[Bis(dimethylamino)methylene]-1H-1,2,3-triazolo[4,5-b]pyridinium 3-oxid hexafluorophosphate (HATU) (0.268 g, 0.70 mmol)

was added. The solution was stirred for one hour before the addition of *N,N*-diisopropylethylamine (DIPEA) (184 µL, 0.137 g, 1.06 mmol) and 1-amino, 5-(2, 3-dibenzyloxybenzamide) pentane (0.160 g, 0.35 mmol) and the mixture stirred overnight. The resulting brown solution was reduced *in vacuo* to a brown residue. The residue was purified twice by column chromatography (1:2 ethyl acetate : chloroform) (1:4 ethyl acetate : chloroform) yielding a white solid product (0.204 g, 0.16 mmol, 55 %) $R_f$ = 0.36 (1:4 ethyl acetate : chloroform) M.P = 96-98 °C. **$^1$H NMR:** (400 MHz, $CDCl_3$) δ: 7.93 (d, *H*6, J = 1.8 Hz, 1H); 7.90 (m, *H*18/24,1H); 7.87 (t, *H*18/24, J = 5.5 Hz, 1H); 7.76 (dd, *H*29/31, J = 6.4 Hz, J = 3.2 Hz, 1H); 7.50-7.14 (m, *H*4/30/9-11/14-16/34-36/39-41/50-52/55-57/60-62/65-67, 42H); 6.98 (m, *H*29/31, 2H); 5.17 (s, *H*12, 2H); 5.11-5.01 (m, *H*32/37, 2H); 5.08 (s, *H*32/37, 2H); 4.98 (br s, *H*7, 2H); 4.95-4.86 (m, *H*48/53, 3H); 4.67-4.56 (m, *H*53/64, 3H); 4.45 (d, *H*47, J = 10.5 Hz, 1H); 4.26 (d, *H*42, J = 9.6 Hz, 1H); 3.86-3.73 (m, *H*47/44/58/46, 5H); 3.63 (dt, *H*45, J = 9.2 Hz, J = 3.2 Hz, 1H); 3.52 (t, *H*43, J = 9.2 Hz, 1H); 3.25-3.18 (m, *H*19, *H*23, 4H); 1.30-1.23 (m, *H*20, *H*22, 4H); 1.16-1.10 (m, H21, 2H). **$^{13}$C NMR:** (100 MHz, $CDCl_3$) δ: 164.9 (*C*17/25); 164.7 (*C*17/25); 151.7 (*C*3/28); 151.4 (*C*3/28); 146.7 (*C*2/27); 146.3 (*C*2/27); 138.7, 138.3, 137.7, 136.4, 136.3, 136.3, 136.3, 135.5 (*C*8/13/33/38/49/54/59/64); 128.8, 128.7, 128.7, 128.6, 128.4, 128.4, 128.2, 128.2, 128.2, 128.0, 127.8, 127.7, 127.6, 127.6, 127.5, 127.5, 127.4, 127.2 (*C*9-11/14-16/34-36/39-41/50-52/55-57/60-62/65-67); 124.4 (*C*4/29/30/31); 123.3 (*C*4/29/30/31); 122.2 (*C*4/29/30/31); 116.8(*C*29/31); 115.8 (*C*6); 86.7 (*C*44/46); 84.0 (*C*43); 81.1 (*C*42); 79.3 (*C*45); 78.3 (*C*44/46); 76.4 (*C*32/37); 75.6 (*C*32/37); 75.1 (*C*48/53); 74.9 (*C*47); 73.4 (*C*53/63); 71.2 (*C*32/37); 71.0 (*C*48/53); 69.1 (*C*58); 39.6 (*C*19/23); 39.5 (*C*19/23); 28.9 (*C*20/22), 28.9 (*C*20/22), 24.5 (C21). **HRMS (ESI):** Calcd. $[M+H]^+$ ($C_{81}H_{80}N_2Na_1O_{11}$) m/z = 1279.5654; Obs. $[M+Na]^+$ m/z = 1279.5606, Mean err 1.9 ppm. **IR ATIR (cm$^{-1}$):** 3384 w br (N-H), 3287 w br (N-H), 3063 w (C-H), 3030 w (C-H), 2920, 2859 w br (C-H), 1638 m (C=O), 1605 w (C=O), 1577 m (C=C ar).

### 1.3.9 5-β-D-glucosyl-5-LICAM (14)

5-β-D-Glucosyl-5-LICAM was prepared based on a literature protocol.[44, 45] 5-Benzyloxy-β-D-glucosyl-3, 4-benzyloxy-4-LICAM (0.200 g, 0.1590 mmol) was dissolved in toluene (1 mL) and ethanol added (30 mL) followed by 3 spatula tips of $Pd(OH)_2$ 20% on carbon. The system was purged with nitrogen before purging with

hydrogen for 30 minutes. The reaction mixture was stirred under balloon pressure of hydrogen for 18 hours, and purged with nitrogen before opening to air. The catalyst was removed by filtration, and the solvent removed *in vacuo* to yield a pale colourless oil. The solid off white product was obtained by cooling the obtained oil in liquid nitrogen and removing all residual solvent *in vacuo* (0.086 g, 0.16 mmol, 90 %). M.P = 180-182 °C. **$^{1}$H NMR:** (400 MHz, MeOD) δ: 7.31 (s, *H*4/6, 1H); 7.20 (d, *H*20/22*,* J= 8.2 Hz 1H); 7.01 (s, *H*4/6, 1H); 6.91 (d, H20/22, J= 7.8 Hz, 1H); 6.70 (t, *H*21, J = 7.8 Hz, 1H); 4.02 (d, *H*26, J = 9.2 Hz, 1H); 3.87 (d, H34, J= 10.5 Hz, 1H); 3.72 (dd, *H*34, $^{2}J_{H34a/H34b}$ = 11.9 Hz, $^{3}J_{H34/H30}$ = 5.0 Hz, 1H); 3.46-3.35 (m, *H*11/15/27-30, 8H); 1.72-1.64 (m, *H*12/14, 4H); 1.50-1.44 (m, *H*13, 2H). **$^{13}$C NMR:** (100 MHz, MeOD) δ: 171.6 (*C*9/17); 171.6 (*C*9/17); 150.4 (*C3/19*); 150.3 (*C3/19*); 147.5 (*C*2/18); 147.1 (*C*2/18); 131.3 (*C*1/23); 119.7 (*C21/*20/22); 119.4 (*C21/*20/22); 118.8 (*C*4/6); 118.1 (*C*20/22); 116.9 (*C*4/6); 116.2 (*C*5); 83.3 (*C*26); 82.1 (*C*27/28/29/30); 79.8 (*C*27/28/29/30); 76.5 (*C*27/28/29/30); 71.8 (*C*27/28/29/30); 63.0 (*C*34); 40.5 (*C*11/15); 40.5 (*C*11/15); 30.3 (*C*12/14); 30.3 (*C*12/14), 25.6 (*C*13). **HRMS (ESI):** Calcd. $[M+H]^{+}$ ($C_{25}H_{32}N_2O_{11}$) m/z = 535.1933; Obs. $[M+H]^{+}$ m/z = 535.1912, Mean err 3.5 ppm. **IR ATIR (cm$^{-1}$):** 3288 s br (O-H), 2930 m br (C-H), 1641 m (C=O), 1589 m (C=C ar). **Elemental Analysis:** Calcd. for [$C_{25}H_{32}N_2O_{11}$.0.9EtOH.1.2$H_2O$]: %C 53.68, %H 6.70, %N 4.66; Measured for [$C_{25}H_{32}N_2O_{11}$.0.9EtOH.1.2$H_2O$]: %C 53.76, %H 6.47, %N 4.52. **Specific Rotation:** $[\alpha]_D$ (Methanol, conc. 0.311 g/100 mL) + 5.7

## 1.4 Jobs Plot

The iron-binding properties of 5-β-D-glucosyl-n-LICAM (n = 4, 5) were investigated *via* a Job plot method.[42] 5-β-D-glucosyl-n-LICAM (n = 4, 5) was combined with varying concentrations of iron(III) to establish preferred metal to ligand binding ratios. The ratios spanned 100% ligand to 100% iron(III), with 5% intervals. Between 60:40 and 50:50 ligand to iron(III) ratios, 2% intervals were used. This protocol resulted in 24 samples over the full range. Stock solutions of 10 mM Fe(III)-nitrilotriacetate (NTA) in $H_2O$ and 10 mM 5-β-D-glucosyl-n-LICAM (n = 4, 5) in DMSO were used in the necessary ratios totalling 200 µL to make up a 2 mL solution of each ratio in 1800 µL 0.11M Tris-HCl pH 7.5, 150 mM NaCl, resulting in an overall iron(III)-ligand concentration of 400 nM. DMSO was kept at 5% v/v for all final solutions. A UV/Vis spectrum from 400 nm to 700 nm was run for each solution after 1 hour of equilibration. The spectra were rerun after 7 days of equilibration. $\lambda_{max}$ values were

monitored at 495 nm and 555 nm and plotted against ligand to protein ratio, and the maximum absorbance for each wavelength recorded at the relevant ligand:protein ratio.

## 1.5 Cloning, expression and purification

CeuE was prepared as previously described.[41, 43] The VctP gene for truncated VctP (residues 51-333), with signal peptide removed, was amplified by PCR from the synthetic DNA purchased from ThermoFisher scientific. Primers used were of the following sequence: FWD_51 TCCAGGGACCAGCAGAGACAGTAACGATTGAACATCGCTTG, REV_333 TGAGGAGAAGGCGCGTTACTGCATACCAACTGACGCTTTCATG. The gene product was directionally cloned into a Lic-adapted pET 28a vector (YSBLic3C), containing a 3C protease cleavable N-terminal hexa-histidine tag, by the In-Fusion method (Clontech). Protein was expressed in *E .coli* strain BL21(DE3). Cells were grown with shaking at 37° in Luria-Bertani broth media containing 30 μg $mL^{-1}$ kanamycin and induced with 1 mM isopropyl β-d-thiogalactopyranoside at an $OD_{600}$ of 0.6-0.8. The cells were harvested by centrifugation 4 hours after induction and resuspended in buffer A (50 mM Tris-HCl, pH 7.8, 500 mM NaCl, 10 mM imidazole) in the presence of protease inhibitor cocktail and lysed by sonication on ice. The soluble crude extract was collected by centrifugation at 19,900 rpm. The standard 3-step procedure was used for VctP purification. Initially a 5 mL His-Trap chelating column (Amersham Pharmacia) was charged with nickel and equilibrated with buffer A. Fractions containing VctP were eluted with buffer B (50 mM Tris-HCl, pH 7.8, 500 mM NaCl, 500 mM imidazole). 3C protease for removal of the histidine tag was added in a 1:50 ratio to an overnight dialysis against buffer C (50 mM Tris-HCl, pH 7.5, 150 mM NaCl). The cleaved sample was loaded in buffer C onto a second His-Trap chelating column, and eluted with buffer B. Non-tagged protein was eluted in the flow-through (FT) fractions which were combined, concentrated by centrifugal ultrafiltration (Amicon Ultra) and purified by gel filtration on a Superdex S200 column in buffer D (50 mM Tris-HCl, pH 8.0; 150 mM NaCl). The final pure sample was concentrated to 90 mg $mL^{-1}$. The molecular mass of the protein was confirmed by electro-spray mass spectrometry.

### 1.6 Fluorescence quenching titrations

Intrinsic fluorescence quenching titrations were carried out as previously described. Spectra were recorded with an excitation of 280 nm, emission range of 295-410 nm, 10 nm excitation slit width, 10 nm emission slit width, 60 nm/min scanning speed, automatic response, corrected spectra and 700 V detector voltage using a Hitachi F-4500 fluorescence spectrophotometer.[42, 43]

### 1.7 Circular Dichroism Spectroscopy

Spectra were recorded in accordance with a published procedure,[43] between 300 nm and 700 nm with data pitch 0.5 mm in continuous scanning mode with speed of 100 nm $min^{-1}$ and response of 2 seconds. The bandwidth was set to 2 nm, with a path length of 1 cm. Spectra were recorded five times and averaged.

Solutions of CeuE and VctP were diluted to $2.5 \times 10^{-3}$ M in 0.11 M Tris-HCl pH 7.5, 150 mM NaCl buffer. A Fe(III)-ligand stock solution containing equimolar NTA was made at a concentration of $5 \times 10^{-4}$ M, by adding 10 µL of both 10 mM ligand in DMSO and 10 µL 10mM Fe(III)-NTA in $H_2O$ to 180 µL 0.11 M Tris-HCl pH 7.5, 150 mM NaCl buffer.

Spectra were recorded of solutions containing 880 µL 0.11 M Tris-HCl pH 7.5, 150 mM NaCl buffer, 100 µL (Fe(III)-ligand NTA stock solution and 20 µL $2.5 \times 10^{-3}$ M CeuE, resulting in a 1:1 ratio of ligand to protein at $5 \times 10^{-5}$ M. The spectrum of buffer was subtracted from all spectra including the spectra for free ligand and apo protein.

## 2 Results and Discussion

### 2.1 Salmochelin mimic synthesis

A salmochelin mimic, Sal-5-LICAM (14), was designed based on a previously studied tetradentate siderophore mimic, 5-LICAM,[43] and synthesised as shown in Scheme 1. The synthesis of aryl *C*-glycosides, such as (12), *via* metal-catalysed cross coupling reactions has previously been described.[44, 45, 50, 51]

To obtain the iodinated intermediate (4) for the cross coupliing coupling step, commercially available (1) was selectively iodinated in the C5 position using iodine monochloride, silver nitrate and pyridine to yield (2),[48] then demethylated *via* $BBr_3$

deprotection (3), followed by benzyl ether protection of both phenolic hydroxyl groups to generate (4) in 51% yield. The acetate protected β-D-glucose unit was then installed at the C5 position *via* Negishi coupling of (4) with acetobromo-α-D-glucose, using a nickel catalyst and conditions adapted from a literature procedure.[44] The activation of (4) using zinc, lithium and iodine in DMF reached completion within an hour and if the reaction mixture was left for 12 hours, as recommended in the literature,[44] decomposition occured. By performing the subsequent Negishi coupling in a glovebox to avoid exposure to the atmosphere, a yield of 66% of (5) was obtained. [44, 45] The acetate protecting groups on the glucose unit were replaced with benzyl groups, yielding two products (6 and 7), which were combined and exposed to sodium hydroxide to afford (12) in 87% yield. Further details and reaction conditions are provided in the experimental section.

In addition, compound 11 was synthesised, to allow for the selective generation of a mono-glucosylated salmochelin mimic. (8) was transformed into (9) *via* standard oxidation and benzyloxy protection reactions. [46] The carboxylic acid of (9) was activated *via* production of the N-hydroxysuccinimide ester (10), [47] which was then coupled with 1, 5-diaminopentane to produce amide bonded (11). The required second amide bond was formed between compounds (11) and (12) *via* a standard HATU coupling reaction yielding (13). Global deprotection of benzyl groups *via* standard hydrogenolysis afforded the target salmochelin-inspired siderophore mimic Sal-5-LICAM (14).

## 2.2 Iron binding by Method of Continuous Variation

Sal-5-LICAM (14) was complexed with iron(III) in varying ligand: iron(III) ratios, and the absorbance spectra recorded (Figure 4A). The $\lambda_{max}$ was observed to shift from around 495 nm to around 555 nm as the Fe(III) to ligand ratio was increased. Plotting the absorbance at 555 nm and 495 nm for each spectrum over the range of ratios, gave the Job plot shown in Figure 4B. The absorbance at 555 nm peaked at a 50:50 ratio, whilst the absorbance at 495 nm peaked at a 60:40 ratio. This indicated that a mixture of 1:1 species and a 3:2 species was present in solution, as represented by the schematic diagram in Figure 4D. After 7 days, the spectra were repeated, to establish whether further equilibration had been taken place. For both wavelengths, the maximum absorbance was achieved at a 60:40 ratio of Sal-5-LICAM : Fe(III) (Figure 4C), which indicated that the 3:2 species is

thermodynamically more stable and predominates over time. Salmochelin siderophores are known to have a reduced membrane partition coefficient when compared to their enterobactin equivalents. [25] It may therefore be that the hydrophilic nature of the glucose moieties and their disposition to hydrogen bond in aqueous solution allows the ligands to assemble and form a 3:2 species with solvent exposed sugars shielding the hydrophobic backbones.[53-54] However, considering the restricted iron levels within the host organism combined with the need for fast bacterial iron uptake, the kinetic 1:1 species is probably biologically more relevant.

## 2.3 Binding of the salmochelin mimic to CeuE

The interactions of the Fe(III) complex of the salmochelin mimic with CeuE were studied by circular dichroism (CD) spectroscopy (Figure 5A). In the absence of protein, no significant signal was observed in the wavelength range of the ligand-to-metal charge transfer band, indicating that a racemic mixture of Λ- and Δ-configured Fe(III) centres was present in solution. However, the CD spectrum obtained in the presence of CeuE shows clear negative bands between 310 and 540 nm and a weak positive band above 550 nm. These bands are indicative of Fe(III)-catecholamide complexes that adopt the Λ-configuration. A similar chiral preference was previously reported for similar bis(catecholate) siderophores and mimics[41-43] and shown by X-ray crystallography to originate from H-bonding and electrostatic interactions with the chiral binding pocket of CeuE and the direct coordination of two amino acid side chains, Tyr288 and His227, to the Fe(III) centre. Hence, the CD spectra confirmed that CeuE is able to bind the Fe(III) complex of the salmochelin S1 mimic and that CeuE shows a preference for Λ-configured coordination centres.

A subsequent fluorescence quenching titration of CeuE with Fe(III)-Sal-5-LICAM (Figure 5B), gave a dissociation constant of 511 ± 76 nM, around 50 times larger than that for the binding of Fe(III)-5-LICAM or the natural siderophore Fe(III)-bisDHBS with CeuE.[42, 43] This suggests that although CeuE is able to bind Fe(III)-Sal-5-LICAM, it appears better suited to the binding of Fe(III)-bisDHBS than salmochelin S1.

## 2.4 Binding of the salmochelin-inspired iron(III)-siderophore mimic to VctP

The CD spectra obtained upon addition of Fe(III)-Sal-5-LICAM to VctP also showed an induced Λ-configuration (Figure 6A). As VctP contains conserved histidine and tyrosine residues, it is likely that the Λ-configured binding mode between Fe(III)-bound tetradentate siderophores is similar in VctP and CeuE. VctP was titrated with Fe(III)-Sal-5-LICAM in triplicate giving a dissociation constant of 9.4 ± 3.0 nM (Figure 6B). Thus VctP binds salmochelin S1 with high affinity, which suggests that *V. cholerae* is able to use the salmochelin stealth siderophores for Fe(III)-uptake via the VctPDGC system.

## 2.5 Comparison of the iron(III)-siderophore binding properties of VctP with those of CeuE

Dissociation constants were measured for VctP titrated with Fe(III)-enterobactin, Fe(III)-bisDHBS, Fe(III)-5-LICAM and compared with those obtained for CeuE (

Table 1). VctP bound Fe(III)-enterobactin with a dissociation constant of 369 ± 25 nM, and with Λ-configured complexes dominating in solution. This affinity was around ten times stronger than that estimated for the binding of CeuE to Fe(III)-enterobactin. The binding of VctP to both Fe(III)-bisDHBS and Fe(III)-5-LICAM was too strong to be quantified *via* fluorescence quenching titrations, due to reaching the limits of detection, and were both estimated to be in the sub-nanomolar range. These results suggest that VctP is able to bind tetradentate catecholate siderophores with very high affinity, including the salmochelin S1 mimic Sal-5-LICAM, but may also be able to use enterobactin for iron uptake in *V. cholerae*. The ability to use both tetradentate and hexadentate catecholate siderophores, as well as stealth siderophores, may contribute to the virulence of *V. cholerae*.

# 3 Summary and conclusions

The salmochelin S1 mimic Sal-5-LICAM was synthesised, characterised and shown to form both 1:1 and 3:2 complexes if equilibrated for one hour ([L] + [M] = 0.4 mM). Similar iron(III)-binding stoichiometries of 1:1 and 3:2 were observed previously with other bis(catecholates), such as 4-LICAM and bisDHBS.[41, 42] Only after a further

equilibration period of seven days was the thermodynamically more stable 3:2 complex seen to predominate. Initial protein-binding studies with diastereoisomeric mixtures of the Fe(III) complexes were carried out by CD spectroscopy and showed that both periplasmic binding proteins, CeuE of *C. jejuni* and VctP of *V. cholerae*, preferentially select for Λ-configured Fe(III) complexes of the salmochelin S1 mimic, as seen previously upon binding of bis(catecholates) to CeuE.[41-43]

Subsequent intrinsic fluorescence quenching titrations revealed that VctP binds the Fe(III) complexes of all catecholate siderophores tested (enterobactin, bisDHBS, 5-LICAM and Sal-5-LICAM) with higher affinity than does CeuE. In addition, both CeuE and VctP display a clear preference for tetradentate bis(catecholates), such as bisDHBS, 5-LICAM and Sal-5-LICAM, over the tris(catecholate) enterobactin. In case of CeuE, the structural basis for this preference for tetradentate siderophores originates from two protein side chains (Tyr288 and His227) that coordinate directly to the Fe(III) centre,[41-43] whilst the coordination of these side chains to Fe(III) enterobactin is not possible, due to a lack of available coordination sites. The observed preference of tetradentate siderophores is also consistent with the report that *V. cholerae* utilises the enterobactin hydrolysis product bisDHBS for the acquisition of Fe(III), but not intact enterobactin.[34] and the finding that bisDHBS is a functional Fe(III) uptake mediator in *C. jejuni*.[55]

Our results suggest that the role of the tetradentate stealth siderophore salmochelin S1 in the iron uptake of enteric pathogens merits further investigation as it may be of importance in iron cross-feeding within environments that are shared with salmochelin-producing *E. coli* strains, for example inflamed mammalian small intestines.[56] Salmochelin S1 utilisation may provide scavenging pathogenic species with a competitive advantage in microbiota where the Fe(III) complexes of enterobactin and vibriobactin are being removed by the innate defence protein siderocalin, whilst glucosylated stealth siderophore, such as salmochelin S1, evade capture.[15-18, 28]

# 4 Acknowledgements

Funding: We would like to thank the EPSRC (grant no. EP/L024829/1, and studentship for E.J.W.) for support.

**Competing interests:** The authors declare no competing interests.

**References**

1. C. Ratledge and L. G. Dover, Annu. Rev. Microbiol. 54 (2000) 881-941.

2. M. L. Guerinot, Annu. Rev. Microbiol. 48 (1994) 743-772.

3. C. Wandersman and P. Delepelaire, Annu. Rev. Microbiol. 58 (2004) 611-647.

4. R. C. Hider and X. Kong, Nat. Prod. Rep. 27 (2010) 637-657.

5. J. R. Butterton and S. B. Calderwood, J. Bacteriol. 176 (1994) 5631-5638.

6. E. E. Wyckoff, A.-M. Valle, S. L. Smith and S. M. Payne, J. Bacteriol. 181 (1999) 7588-7596.

7. E. E. Wyckoff, A. R. Mey and S. M. Payne, Biometals 20 (2007) 405-416.

8. B. E. Allred, T. Hoette and K. N. Raymond, Abstr. Pap. Am. Chem. Soc., 239 (2010) 1.

9. T. M. Hoette, R. J. Abergel, J. D. Xu, R. K. Strong and K. N. Raymond, J. Am. Chem. Soc. 130 (2008) 17584-17592.

10. R. J. Abergel, M. C. Clifton, J. C. Pizarro, J. A. Warner, D. K. Shuh, R. K. Strong and K. N. Raymond, J. Am. Chem. Soc. 130 (2008) 11524-11534.

11. M. A. Holmes, W. Paulsene, X. Jide, C. Ratledge and R. K. Strong, Structure 13 (2005) 29-41.

12. B. E. Allred, P. B. Rupert, S. S. Gauny, D. D. An, C. Y. Ralston, M. Sturzbecher-Hoehne, R. K. Strong and R. J. Abergel, Proc. Natl. Acad. Sci. 112 (2015) 10342-10347.

13. B. E. Allred, C. Correnti, M. C. Clifton, R. K. Strong and K. N. Raymond, ACS Chem. Biol. 8 (2013) 1882-1887.

14. G. Bao, M. Clifton, T. M. Hoette, K. Mori, S.-X. Deng, A. Qiu, M. Viltard, D. Williams, N. Paragas, T. Leete, R. Kulkarni, X. Li, B. Lee, A. Kalandadze, A. J. Ratner, J. C. Pizarro, K. M. Schmidt-Ott, D. W. Landry, K. N. Raymond, R. K. Strong and J. Barasch, Nat. Chem. Biol., 6 (2010) 602-609.

15. D. H. Goetz, M. A. Holmes, N. Borregaard, M. E. Bluhm, K. N. Raymond and R. K. Strong, Mol. Cell 10 (2002) 1033-1043.

16. E. P. Skaar, Cell Host Microbe 5 (2009) 422-424.

17. A. K. Sia, B. E. Allred and K. N. Raymond, Curr. Opin. Chem. Biol. 17 (2013) 150-157.

18. E. P. Skaar, PLOS Pathogens 6 (2010) e1000949.

19. M. Caza, A. Garenaux, F. Lepine and C. M. Dozois, Molec. Microbiol. 97 (2015) 717-732.

20. M. Valdebenito, B. Bister, R. Reissbrodt, K. Hantke and G. Winkelmann, Int. J. Med. Microbiol. 295 (2005) 99-107.

21. M. Valdebenito, A. L. Crumbliss, G. Winkelmann and K. Hantke, Int. J. Med. Microbiol. 296 (2006) 513-520.

22. M. G. Zhu, M. Valdebenito, G. Winkelmann and K. Hantke, Microbiology 151 (2005) 2363-2372.

23. S. I. Elshahawi, K. A. Shaaban, M. K. Kharel and J. S. Thorson, Chem. Soc. Rev. 44 (2015) 7591-7697.

24. B. Bister, D. Bischoff, G. Nicholson, M. Valdebenito, K. Schneider, G. Winkelmann, K. Hantke and R. Süssmuth, Biometals 17 (2004) 471-481.

25. M. Luo, H. Lin, M. A. Fischbach, D. R. Liu, C. T. Walsh and J. T. Groves, ACS Chem. Biol. 1 (2006) 29-32.

26. K. Hantke, G. Nicholson, W. Rabsch and G. Winkelmann, Proc. Natl. Acad. Sci. 100 (2003) 3677-3682.

27. S. Muller, M. Valdebenito and K. Hantke, Biometals 22 (2009) 691-695.

28. A. L. Nelson, J. M. Barasch, R. M. Bunte and J. N. Weiser, Cell. Microbiol. 7 (2005) 1404-1417.

29. S. M. Faruque, M. J. Albert and J. J. Mekalanos, Microbiol. Mol. Biol. Rev. 62 (1998) 1301-1314.

30. D. A. Sack and S. R Bradley Sack MD, N. Engl. J. Med. 355 (2006) 649-651.

31. A. R. Mey, E. E. Wyckoff, A. G. Oglesby, E. Rab, R. K. Taylor and S. M. Payne, Infect. Immun. 70 (2002) 3419-3426.

32. E. E. Wyckoff, A. R. Mey, A. Leimbach, C. F. Fisher and S. M. Payne, J. Bacteriol. 188 (2006) 6515-6523.

33. E. E. Wyckoff and S. M. Payne, Molec. Microbiol. 81 (2011) 1446-1458.

34. E. E. Wyckoff, B. E. Allred, K. N. Raymond and S. M. Payne, J. Bacteriol. 197 (2015) 2840-2849.

35. J. Rutz, T. Abdullah, S. Singh, V. Kalve and P. Klebba, J. Bacteriol. 173 (1991) 5964-5974.

36. S. S. Seliger, A. R. Mey, A. M. Valle and S. M. Payne, Molec. Microbiol. 39 (2001) 801-812.

37. S. M. Payne, A. R. Mey and E. E. Wyckoff, Microbiol. Mol. Biol. Rev. 80 (2016) 69-90.

38. J. R. Butterton, J. A. Stoebner, S. M. Payne and S. B. Calderwood, J. Bacteriol. 174 (1992) 3729-3738.

39. N. Li, C. Zhang, B. Li, X. Liu, Y. Huang, S. Xu and L. Gu, J. Biol. Chem. 287 (2012) 8912-8919.

40. X. Liu, Q. Du, Z. Wang, S. Liu, N. Li, Y. Chen, C. Zhu, D. Zhu, T. Wei and Y. Huang, FEBS Lett. 586 (2012) 1240-1244.

41. D. J. Raines, O. V. Moroz, K. S. Wilson and A. K. Duhme-Klair, Angew. Chem., Int. Ed. Engl. 52 (2013) 4595-4598.

42. D. J. Raines, O. V. Moroz, E. V. Blagova, J. P. Turkenburg, K. S. Wilson and A.-K. Duhme-Klair, Proc. Natl. Acad. Sci. 113 (2016) 5850–5855.

43. E. J. Wilde, A. Hughes, E. V. Blagova, O. V. Moroz, R. P. Thomas, J. P. Turkenburg, D. J. Raines, A.-K. Duhme-Klair and K. S. Wilson, Sci. Rep. 7 (2017) 45941-45955.

44. H. G. Gong and M. R. Gagne, J. Am. Chem. Soc. 130 (2008) 12177-12183.

45. X. Yu, Y. Dai, T. Yang, M. R. Gagné and H. Gong, Tetrahedron 67 (2011) 144-151.

46. W. H. Rastetter, T. J. Erickson and M. C. Venuti, J. Org. Chem. 46 (1981) 3579-3590.

47. A. Chimiak and J. B. Neilands, in Siderophores from Microorganisms and Plants, Springer Berlin Heidelberg, Berlin, Heidelberg, 1984, pp. 89-96.

48. A. V. Joshua, S. K. Sharma and D. N. Abrams, Synth. Commun. 38 (2008) 434-440.

49. A.-K. Duhme, Z. Dauter, R. C. Hider and S. Pohl, Inorg. Chem. 35 (1996) 3059-3061.

50. F. Zhu, J. Rodriguez, T. Yang, I. Kevlishvili, E. Miller, D. Yi, S. O'Neill,

M. J. Rourke, P. Liu, and M. A. Walczak, J. Am. Chem. Soc. 139 (2017) 17908-17922.

51. L. Adak, S. Kawamura, G. Toma, T. Takenaka, K. Isozaki, H. Takaya, A. Orita, H. C. Li, T. K. M. Shing and M. Nakamura, J. Am. Chem. Soc. 139 (2017) 10693-10701.

52. F. M. Raymo and J. F. Stoddart, Chem. Ber. 129 (1996) 981-990.

53. M. L. Saha, S. De, S. Pramanik and M. Schmittel, Chem. Soc. Rev. 42 (2013) 6860-6909.

54. M. Albrecht, Chem. Rev. 101 (2001) 3457-3498.

55. C. Y. Zamora, A. G. E. Madec, W. Neumann, E. M. Nolan, B. Imperiali, Bioorg. Med. Chem., 2018, in press, https://doi.org/10.1016/j.bmc.2018.04.030.

56. G. A. M. Kortman, M. Raffatellu, D. W. Swinkels and H. Tjalsma, FEMS Microbiol. Rev. 38 (2014) 1202-1234.

Table 1: Dissociation constants for CeuE and VctP with a selection of Fe(III)-siderophores and Fe(III)-siderophore mimics, as determined by fluorescence quenching titrations.

| **Fe(III)-Ligand** | **CeuE $K_d$ /nM** | **VctP $K_d$ /nM** |
|---|---|---|
| **Enterobactin** | 3500 ± 300 | 369 ± 25 |
| **bisDHBS** | 10.1 ± 3.8 (lit.[42]) | <1 |
| **5-LICAM** | <10 (lit.[43]) | <1 |
| **Sal-5-LICAM** | 511 ± 76 | 9.4 ± 3.0 |
| 40 mM Tris-HCl buffer, pH 7.5, 150 mM NaCl, titrations were performed as independent triplicates, with the uncertainty in the average shown. | | |

Figure and scheme captions:

Figure 1: Catecholate siderophores used by *Vibrio cholerae* for iron(III)-uptake.[7]

Figure 2: Salmochelin siderophores.[24]

Figure 3: Known functions of proteins involved in Fe(III) catecholate siderophore uptake in *V. cholerae*. Uptake through the outer membrane is mediated by the outer membrane receptors VctA, IrgA and ViuA, which are energised by the TonB-ExbB-ExbD complex. Periplasmic binding proteins (VctP, ViuP) capture the Fe(III) siderophore complexes in the periplasm for subsequent uptake through the inner membrane transporters VctDG, VctC, ViuDG and ViuC. In the cytoplasm, ViuB facilitates the release of the iron form its siderophore complex *via* reduction of Fe(III)

to Fe(II). Ent = enterobactin, Vib = vibriobactin, trisDHBS = tris(2, 3-dihydroxybenzoyl-L-serine), bisDHBS = bis(2, 3-dihydroxybenzoyl-L-serine).

Figure 4: Selected electronic absorbance spectra obtained at the indicated metal-to-ligand ratios; [M]+[L] = 0.4 mM; 0.1 M Tris-HCl; 150 mM NaCl; 5% v/v DMSO; pH 7.5 (A), Job plots (B: 1 hour C: 7 days) for the reaction of Sal-5-LICAM with iron(III), and schematic representation of a 1:1 and 3:2 tetradentate ligand : iron complex (D) (solvent molecules are depicted as Sol).

Figure 5: A: CD spectra for Fe(III)-Sal-5-LICAM, showing some induced Λ-configuration upon complexation with CeuE. B: Fluorescence quenching titration curves (in triplicate) obtained with CeuE and Fe(III)-Sal-5-LICAM.

Figure 6: A: CD spectra for Fe(III)-Sal-5-LICAM, showing Λ-configuration upon binding to VctP. B: Triplicate binding curves for fluorescence quenching titration of VctP with Fe(III)-Sal-5-LICAM.

Scheme 1: Synthesis of Sal-5-LICAM (14) a: $AgNO_3$, ICl, Pyridine, $CHCl_3$ b: 1) $BBr_3$, DCM 2) $H_2SO_4$, MeOH, 75 ºC c: BnBr, NaI, DMF d: 1-Bromo-α-D-glucose tetraacetate, Zn, LiCl, $Ni(COD)_2$, $^tBu$Terpy, DMF e: 1) $Na_2CO_3$, MeOH 2) BnBr, NaH, $Bu_4NI$, DMF f: NaOH, THF, MeOH g: 1) BnCl, $K_2CO_3$, EtOH 2) $H_3NSO_3$, $NaClO_3$, Acetone, $H_2O$ h: N-hydroxysuccinimide, DCC, Dioxane i:1,5-diaminopentane, $Et_3N$, THF j: HATU, $Et_3N$, DMF k: $H_2$, $Pd(OH)_2$/C 10%, EtOH/Toluene.

**Figures and schemes:**

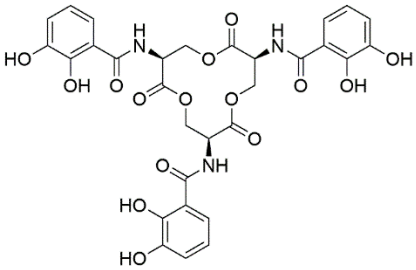

**Enterobactin**

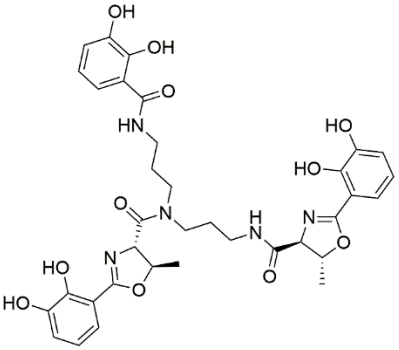

**Vibriobactin**

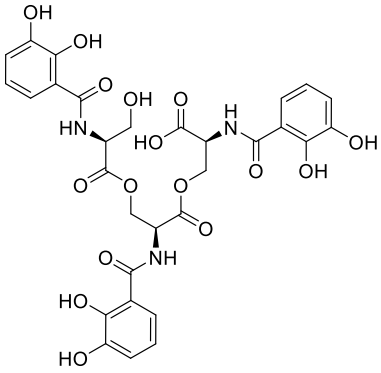

**Tris(2, 3-dihydroxybenzoyl-L-serine),TrisDHBS**

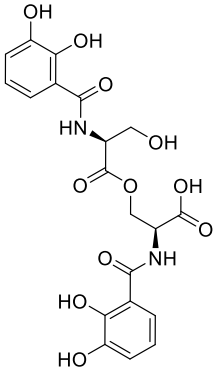

**Bis(2, 3-dihydroxybenzoyl-L-serine), BisDHBS**

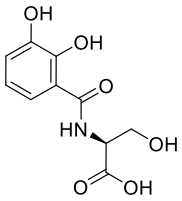

**2, 3-dihydroxybenzoyl-L-serine, DHBS**

Figure 1

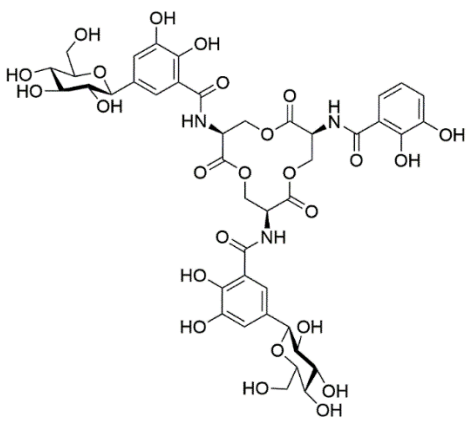

**Salmochelin S4**

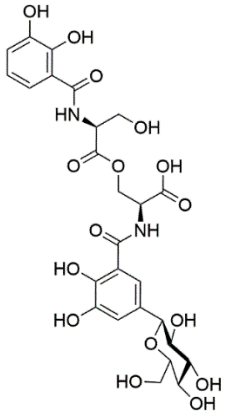

**Salmochelin S1**

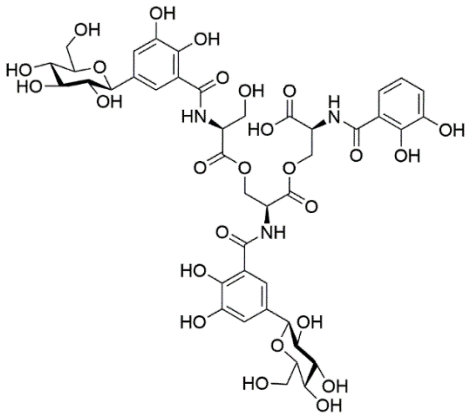

**Salmochelin S2**

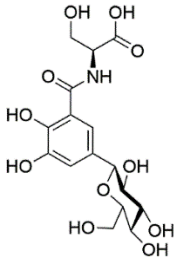

**Salmochelin SX**

Figure 2

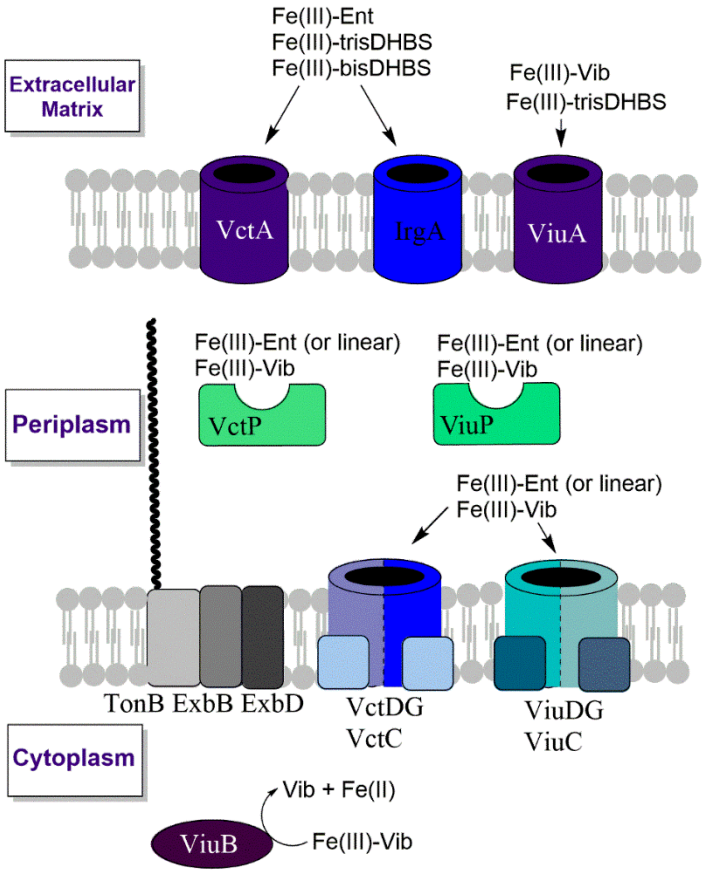
Fe(III)-Ent
Fe(III)-trisDHBS
Fe(III)-bisDHBS
Fe(III)-Vib
Fe(III)-trisDHBS
Extracellular Matrix
VctA
IrgA
ViuA
Fe(III)-Ent (or linear)
Fe(III)-Vib
Fe(III)-Ent (or linear)
Fe(III)-Vib
Periplasm
VctP
ViuP
Fe(III)-Ent (or linear)
Fe(III)-Vib
TonB ExbB ExbD
VctDG
VctC
ViuDG
ViuC
Cytoplasm
Vib + Fe(II)
ViuB
Fe(III)-Vib

Figure 3

A

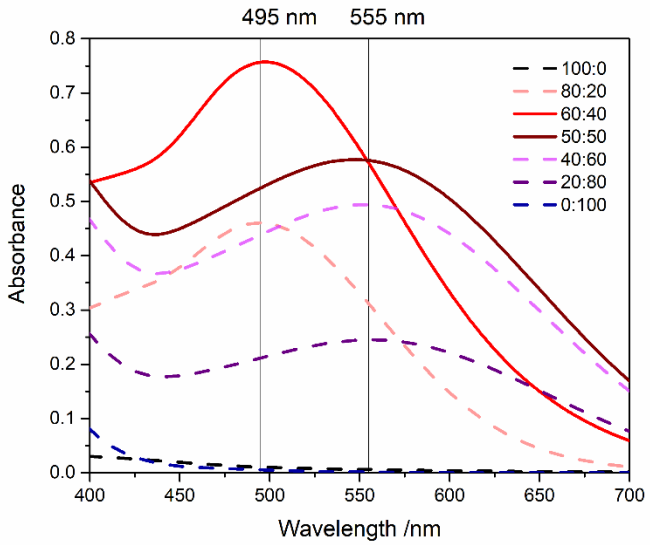
495 nm
555 nm
100:0
80:20
60:40
50:50
40:60
20:80
0:100
Absorbance
Wavelength /nm

B

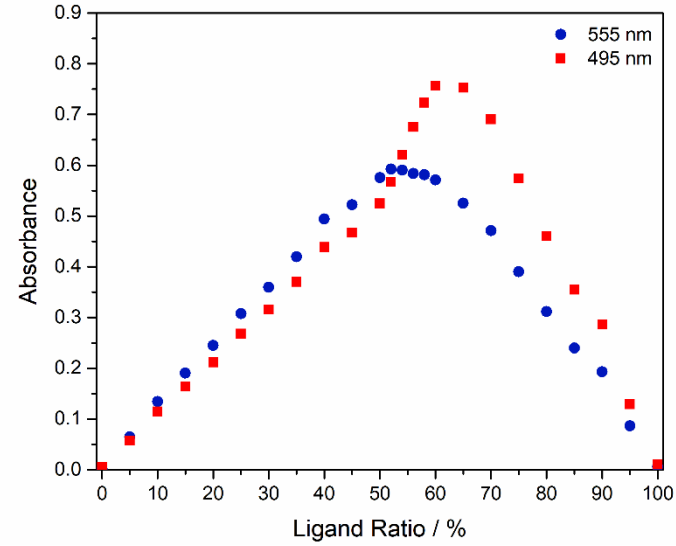
555 nm
495 nm
Absorbance
Ligand Ratio / %

C

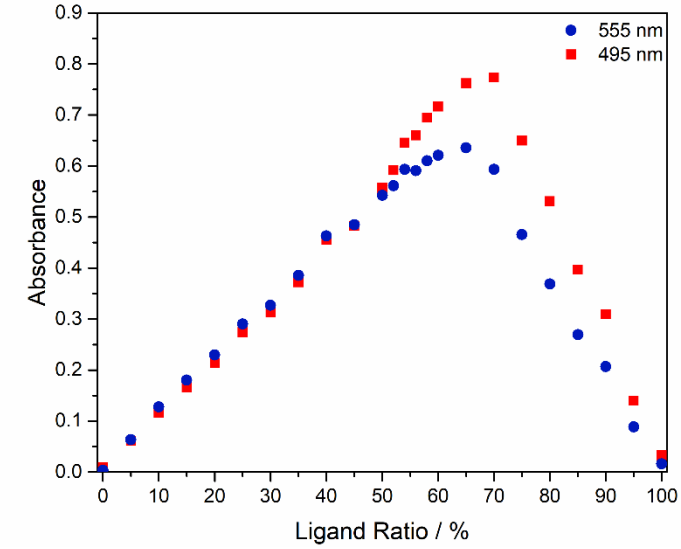
555 nm
495 nm
Absorbance
Ligand Ratio / %

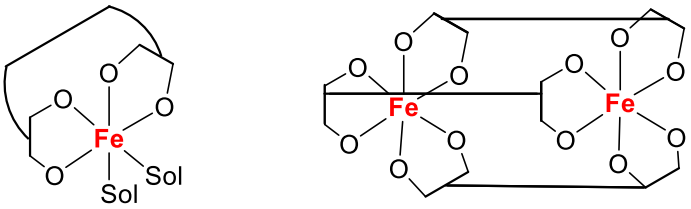


1 : 1 3 : 2

Figure 4

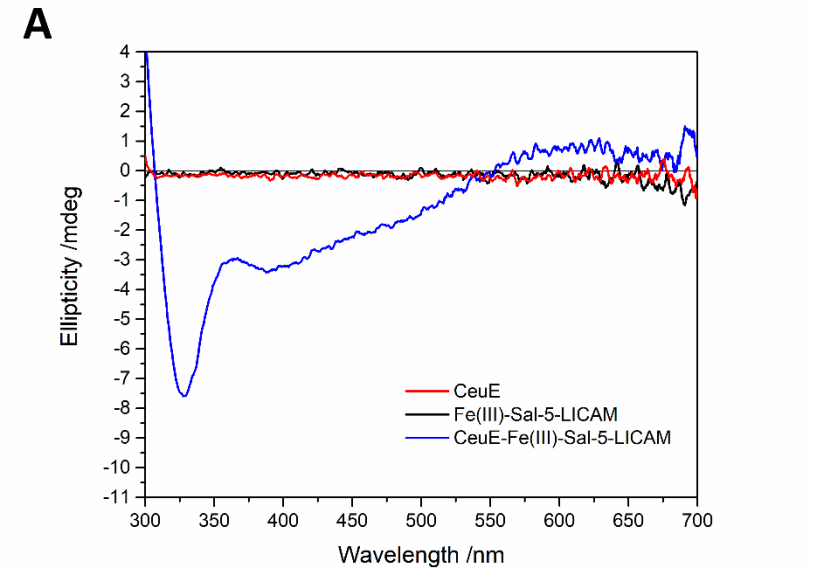


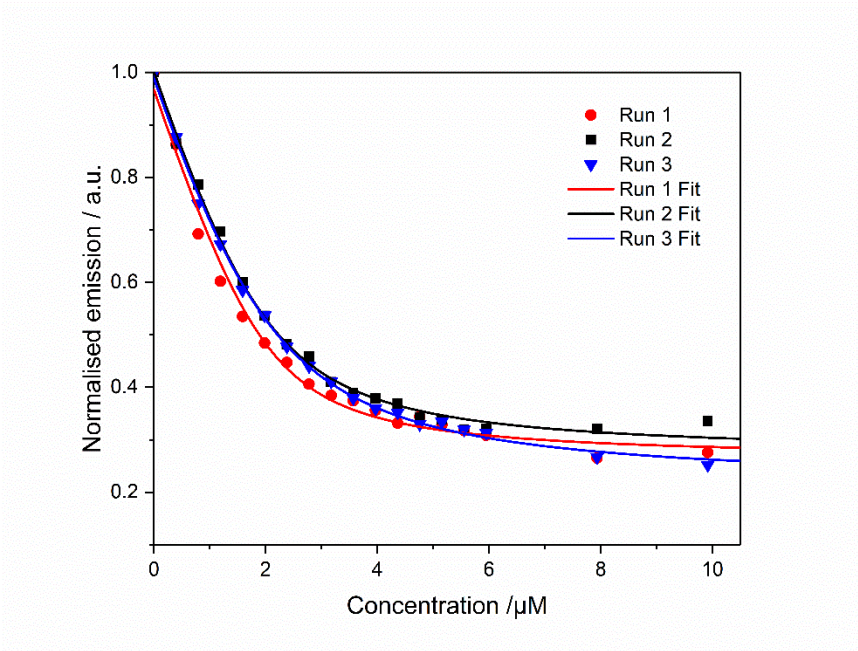


Figure 5

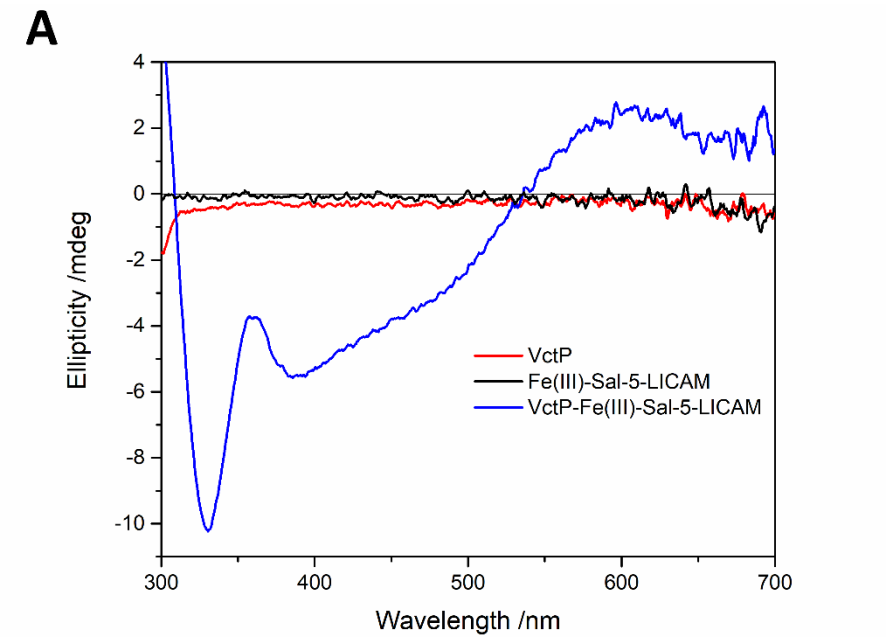
A
Ellipticity /mdeg
Wavelength /nm
VctP
Fe(III)-Sal-5-LICAM
VctP-Fe(III)-Sal-5-LICAM

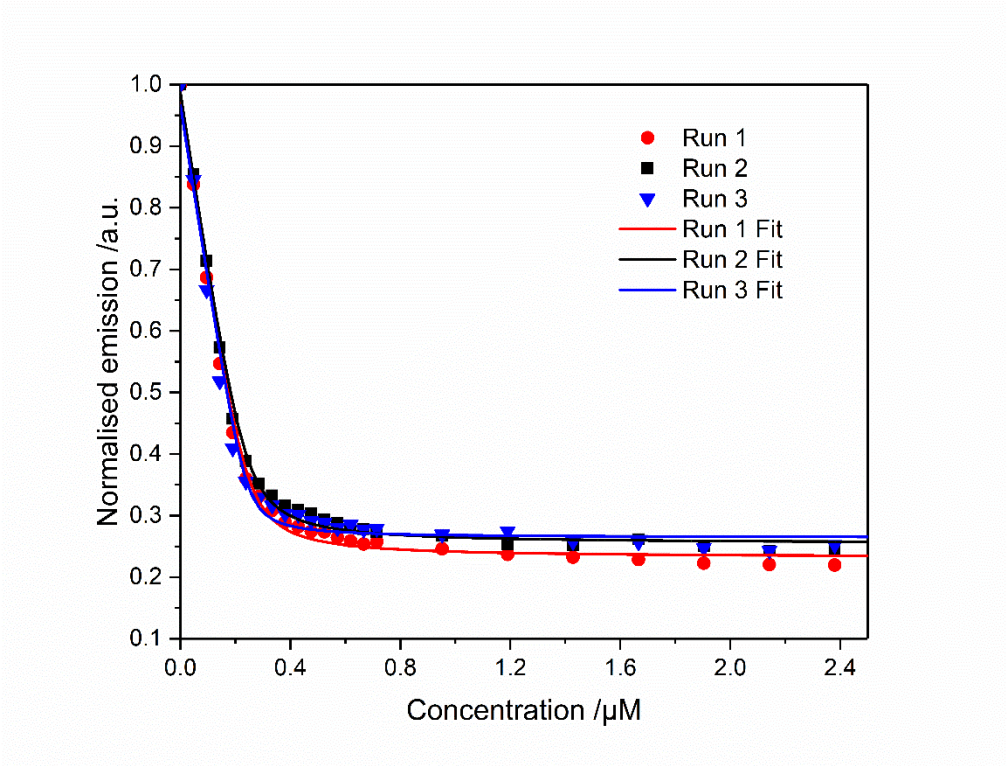
Normalised emission /a.u.
Concentration /μM
Run 1
Run 2
Run 3
Run 1 Fit
Run 2 Fit
Run 3 Fit

Figure 6

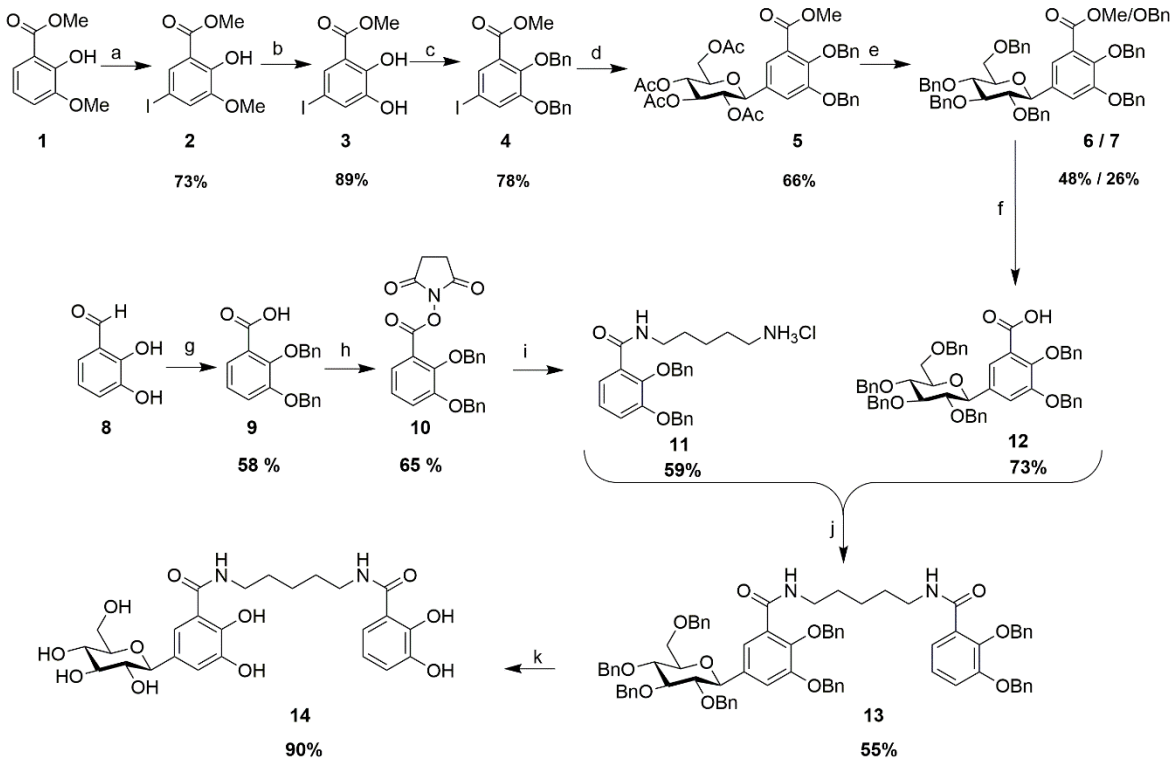


Scheme 1